

# THE ARAUCARIA PROJECT. VLT SPECTRA OF BLUE SUPERGIANTS IN WLM<sup>1</sup>: CLASSIFICATION AND FIRST ABUNDANCES

FABIO BRESOLIN

Institute for Astronomy, 2680 Woodlawn Drive, Honolulu, HI 96822; bresolin@ifa.hawaii.edu

GRZEGORZ PIETRZYŃSKI

Universidad de Concepción, Departamento de Física, Casilla 160-C, Concepción, Chile; pietrzn@hubble.cfm.udec.cl

MIGUEL A. URBANEJA

Institute for Astronomy, 2680 Woodlawn Drive, Honolulu, HI 96822; urbaneja@ifa.hawaii.edu

WOLFGANG GIEREN

Universidad de Concepción, Departamento de Física, Casilla 160-C, Concepción, Chile; wgieren@coma.cfm.udec.cl

ROLF-PETER KUDRITZKI

Institute for Astronomy, 2680 Woodlawn Drive, Honolulu, HI 96822; kud@ifa.hawaii.edu

AND

KIM A. VENN

Department of Physics & Astronomy, University of Victoria, 3800 Finnerty Road, Victoria, BC V8P 1A1, Canada; venn@clare.phys.uvic.ca

## ABSTRACT

As part of the Araucaria Project, we present the first spectral catalog of supergiant stars in the Local Group dwarf irregular galaxy WLM. In assigning a spectral classification to these stars we accounted for the low metal content of WLM relative to the galactic standards used in the MK process, by using classification criteria developed for B and A supergiants contained in the Small Magellanic Cloud. Our spectral catalog shows that our higher S/N spectroscopic sample of 19 objects contains at least 6 early-B (B0-B5) supergiants and 6 late-B and early-A (B8-A2) stars of luminosity class between Ia and II, as well as an O7 V star and an O9.7 Ia star. The spectra of several of these stars is of sufficiently high quality for a determination of the stellar parameters and abundances. We have acquired also a second set of lower S/N spectra for mostly BA stars, however their quality does not allow a further analysis. We have carried out a quantitative analysis for three early-B supergiants. The mean oxygen abundance we derive is  $12 + \log(\text{O}/\text{H}) = 7.83 \pm 0.12$ . This value agrees very well with the measurement that is obtained from H II regions. We therefore find no additional evidence for the discrepancy between stellar and nebular oxygen abundances measured for a single A-type supergiant by Venn et al. The analysis of B- and A-type supergiants yields compatible results for nitrogen, silicon and magnesium. We show that the photometric variability of the blue supergiants included in our spectroscopic sample is negligible for the use of these stars as distance indicators.

*Subject headings:* galaxies: abundances — galaxies: stellar content — galaxies: individual (WLM) — stars: early-type

## 1. INTRODUCTION

Blue supergiant stars can be observed spectroscopically with current telescopes at distances of a few Mpc, reaching outside of the Local Group. This has been possible only since recent times (Bresolin et al. 2001), allowing to collect information on the physical properties and the chemical compositions of large samples of massive stars in different galactic environments. To achieve this goal, multi-object spectroscopy at moderate spectral resolution (Bresolin et al. 2002) provides an effective complement to the detailed spectral analysis of individual supergiants feasible from high-resolution spectra out to distances of  $\sim 1$  Mpc (Venn et al. 2001, Kaufer et al. 2004).

A number of open issues linked to the investigation of the surface chemical composition of massive stars benefit from new spectroscopic observations in the optical range of large

samples of BA supergiants in nearby galaxies. These include the efforts to constrain mixing and wind properties in current models of stellar evolution (Trundle & Lennon 2005), and to probe abundance gradients of various chemical elements in spiral galaxies in the context of galactic chemical evolution (Urbaneja et al. 2005a). In connection to the latter point, recently (Urbaneja et al. 2005b) the analysis of blue supergiants has started to provide important checks on the oxygen abundances derived from H II regions in the central regions of spiral galaxies, where measurements of electron temperatures of the ionized gas suggest a major downward revision of the nebular metal abundances (Bresolin et al. 2004a, 2005).

As part of the Araucaria Project (Gieren et al. 2005) we have obtained spectra of blue supergiants in galaxies of the Local Group or its immediate vicinities (WLM, NGC 6822, IC 1613, NGC 3109) and of the Sculptor Group (NGC 55, NGC 247, NGC 300, NGC 7793) with the ESO VLT tele-

<sup>1</sup> Based on VLT observations for ESO Large Programme 171.D-0004.

scope and its FORS spectrograph. The spectra obtained in NGC 300 (Bresolin et al. 2002) have led to the first determination of the abundance gradient of  $\alpha$ -elements for a spiral galaxy located beyond the Local Group (Urbaneja et al. 2005b). Moreover, utilizing the same data Kudritzki et al. (2003) showed that the stellar parameters ( $T_{\text{eff}}$ ,  $\log g$ ) derived from the spectra of BA supergiants in NGC 300 define a tight relation with the stellar luminosity:  $M_{\text{bol}} = a \log(g/T_{\text{eff}}^4) + b$ . This Flux-weighted gravity–Luminosity Relationship (FGLR) is followed by supergiant stars in a number of additional galaxies, and is being used in the Araucaria Project, in combination with other stellar distance indicators, to remove the potential effect that metallicity has on the derivation of extragalactic distances from the Cepheid Period-Luminosity relation.

With a total absolute magnitude  $M_B \simeq -14.0$ , WLM is one of the faintest dwarf irregular galaxies in the Local Group. The distance to WLM has been measured by several authors using different stellar indicators. We will adopt the recent determination by McConnachie et al. (2005) based on the Tip of the Red Giant Branch (TRGB):  $(m-M)_0 = 24.85 \pm 0.08$ , corresponding to  $932 \pm 33$  Kpc. The values measured by Minniti & Zijlstra (1997) via the TRGB method, by Dolphin (2000) from a fit to the color-magnitude diagram and by Rejkuba et al. (2000) from the magnitude of the horizontal branch are all consistent with the latest TRGB result. The early Cepheid distance by Sandage & Carlson (1985), who detected 15 of these variables, suffered from an inaccurate calibration of their photographic photometry (Ferraro et al. 1989). The Cepheid distance quoted by Lee et al. (1993) is in agreement with the other techniques. Several new Cepheids have been discovered in the course of the Araucaria Project, and a distance based on the optical and near-infrared Period-Luminosity relation is in preparation by our group. The stellar photometric studies mentioned above consistently derive a low value for the reddening across the disk of WLM, with little indication for differential extinction. McConnachie et al. (2005) report  $E(B-V) = 0.035$ , which is in fact the simple foreground component (Schlegel et al. 1998).

CCD photometry has shown that WLM possesses a young population concentrated in the disk of the galaxy, superimposed on an old and extended metal-poor halo (Ferraro et al. 1989, Minniti & Zijlstra 1996, 1997). A metallicity of the old component  $[\text{Fe}/\text{H}] = -1.45$  has been derived from the color of the Red Giant Branch (Minniti & Zijlstra 1997, McConnachie et al. 2005). Within the uncertainties, this is consistent with the calculation of Dolphin (2000) for the metallicity at the end of the initial episode of star formation in WLM, derived from the color-magnitude diagram based on Hubble Space Telescope WFPC2 photometry. The present-day metallicity has been measured from a few H II regions by Skillman et al. (1989b), Hodge & Miller (1995) and Lee et al. (2005). These authors consistently obtained a low oxygen abundance, based on the electron temperature measured from the  $[\text{O III}]\lambda 4363$  line in two of the brightest nebulae. The value reported by Lee et al. (2005),  $12 + \log(\text{O}/\text{H}) = 7.83 \pm 0.06$ , corresponds to 15% of the solar value  $[12 + \log(\text{O}/\text{H})_{\odot} = 8.66$ , Asplund et al. 2004). This low nebular oxygen abundance,  $[\text{O}/\text{H}] = -0.83 \text{ dex}^2$ , while fitting the luminosity-metallicity relationship for dwarf irregular galaxies (Skillman et al. 1989a), contrasts with the re-

sult obtained for an A-type supergiant,  $[\text{O}/\text{H}] = -0.21 \text{ dex}$ , by Venn et al. (2003). This discrepancy between stellar and nebular chemical compositions is the first of its kind so far detected in a dwarf irregular galaxy, and clearly warrants further investigation. An apparent mismatch between stellar and nebular abundances has been noted also in the spiral galaxy M31 (Trundle et al. 2002), but the H II region oxygen abundances in this galaxy are very uncertain, and the amount (or even existence) of the discrepancy heavily depends on which calibration for the strong-line abundance diagnostic  $R_{23}$  (Pagel et al. 1979) is adopted. In WLM, on the other hand, the problem is more severe, because the nebular abundances are much more reliable, being based on the direct measurement of the electron temperature.

In this paper we focus on the brightest blue stars of WLM, centrally located in the disk of the galaxy, where recent low-level star formation has occurred, as also indicated by the presence of gas photoionized by massive stars. We present spectroscopy of 38 stars distributed across the disk of WLM. Several reasons make this galaxy an interesting target for a spectroscopic investigation of its blue supergiant content: (1) the spectral classification and the derivation of stellar parameters at low metallicity; (2) the measurement of stellar chemical abundances, to be compared with the results from nebular studies; (3) the possibility of testing the FGLR method at a significant distance of  $\sim 1$  Mpc. In the current paper we address the first two points, by assigning a spectral classification to our spectroscopic targets, and by measuring the chemical abundances of three early-B supergiants. The investigation of the metallicity of late-B and early-A stars and of the FGLR in WLM is deferred to a future paper, that will follow the publication of a stellar continuum-fitting technique we are developing. In the current paper we discuss the observational data and their reduction in § 2. We present the spectral catalog for our sample in § 3. In § 4 we derive the chemical abundances for early-B supergiants, and compare them with the nebular abundances obtained in WLM. In § 5 we discuss the photometric variability of the spectroscopic targets, and conclude with a summary in § 6.

## 2. OBSERVATIONS

Spectra of blue supergiant candidates in WLM have been acquired at the Very Large Telescope UT4 (Yepun) with the Focal Reducer and low dispersion Spectrograph 2 (FOR2) in MOS mode. Candidates for this study were selected on the basis of their  $V-I$  color index and  $V$  magnitude, measured from the photometry obtained as part of our Cepheid variable search program at the Las Campanas Polish 1.3m telescope (Pietrzyński et al. 2006, in preparation; see Pietrzyński et al. 2002 for details on the data reduction). A large fraction of our targets are included in the Sandage & Carlson (1985) list of bright blue stars (the SC numbers in Table 1). We also included in the sample the A-type supergiant SC 15 analyzed by Venn et al. (2003), as well as the early-B star SC 35, for which these authors could not measure  $T_{\text{eff}}$ , because of the unavailability of the Si III diagnostic in their spectrum. We have compared the  $V$  magnitudes of our targets with the photometry of McConnachie et al. (2005). The agreement between 35 objects in common, in the order of 0.01 mag or better, with no significant zero-point offset, is excellent and in line with other comparisons published in our series of papers (e.g. Pietrzyński et al. 2002, 2004).

The spectra were acquired on two separate nights: July 28 and October 26, 2003. On both nights, we obtained spec-

<sup>2</sup> Logarithmic abundance relative to the solar value:  $[\text{O}/\text{H}] = \log(\text{O}/\text{H}) - \log(\text{O}/\text{H})_{\odot}$ .

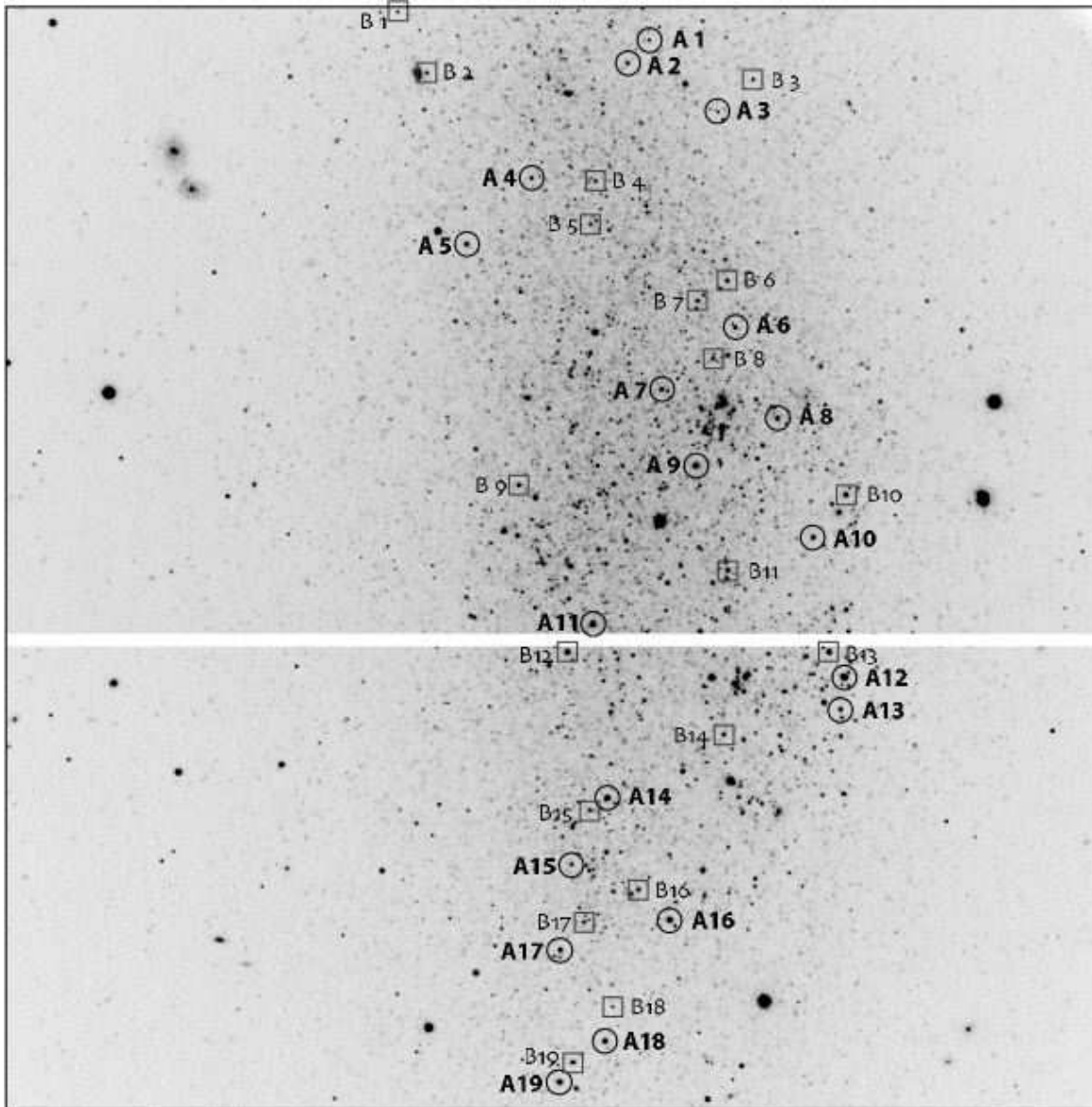


FIG. 1.— We obtained multi-object spectroscopy of WLM supergiant candidates with two different slit setups. In this FORS2 image, used for these setups, we indicate with circles the targets observed in July 2003 (set A) and with squares those observed in October 2003 (set B). The targets are numbered in progressive order, starting from the top of the image. The white horizontal band corresponds to the gap in the FORS2 CCD mosaic, as projected on the sky. North is up and East is to the left.

tra of 19 stars with the 600B grism, achieving a resolution of  $\sim 5 \text{ \AA}$ . The airmass during the observations was smaller than 1.07. The spectra span approximately 2500 angstroms on the  $2048 \times 4096$  FORS2 mosaic, centered around  $4500 \text{ \AA}$ . The stellar targets for the two sets of observations (denoted with the letters A and B in the remainder of the paper for the July and October runs, respectively) are positioned in the same section of the galaxy, where young stars and H II regions are concentrated (see Fig. 1). Our set B includes stars that received lower priority during our target selection, either because of their fainter magnitudes or because of the higher probability for the presence of neighboring stars, that might contaminate the spectra. We must also mention the fact that at the northern and southern extremes of the observed field no suitable blue supergiant candidate was available. In these cases we obtained spectra of bright red stellar objects. The location of the spectroscopic targets in the  $V$  vs  $V - I$  color-

magnitude diagram is shown in Fig. 2.

The total exposure times were 4500 seconds (set A) and 3600 seconds (set B). The seeing was good throughout the first night ( $0''.7$ ), but only mediocre ( $1''.2$ ) during the second. Correspondingly, the signal-to-noise ratio (S/N) for our second set of spectra is not sufficiently high ( $S/N = 20\text{--}40$  in most cases) to allow a quantitative analysis for an accurate derivation of the stellar parameters. For set A, on the other hand, the S/N per pixel at  $4500 \text{ \AA}$  is larger than 40 for all but four stars, reaching a maximum of  $\sim 120$ .

Although rectified spectra are generally sufficient for the derivation of chemical abundances and stellar parameters, we also decided to flux calibrate the stellar spectra. For this purpose the spectrophotometric standards Feige 110, CD-32 9927 and LTT 4816 were observed. The spectral energy distributions thus obtained will be used, in conjunction with the line features and model spectra, to constrain the stellar

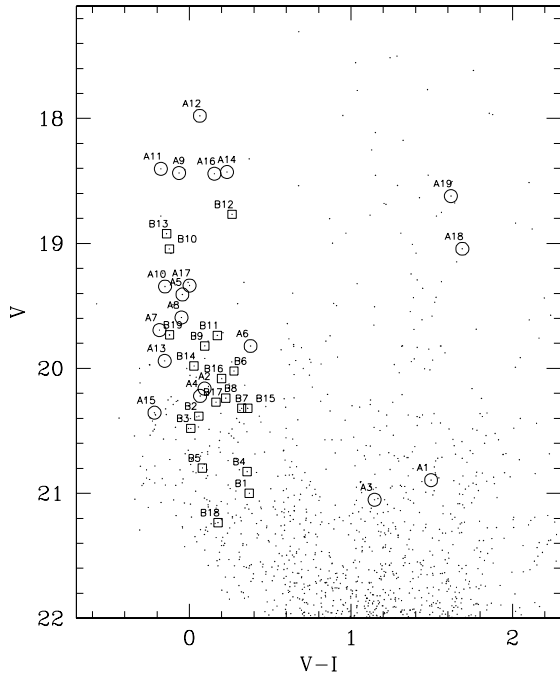


FIG. 2.— The stars for which we have obtained spectra indicated on the  $V$  vs  $V-I$  color-magnitude diagram.

parameters in a future paper on the FGLR.

The two frames available in each field were combined, in order to increase the S/N ratio. We extracted the individual 2-D spectra (extending  $\sim 20$  arcsec along the spatial direction), corresponding to each of the 19 slitlets, from the average images and proceeded by utilizing common IRAF tasks for longslit spectroscopy data reduction. These included bias and flat-fielding corrections, cosmic ray rejection and wavelength calibration via He+HgCd lamp exposures. We finally obtained sky-subtracted 1-D spectra, normalized using a low-order polynomial. A flux-calibrated version of the extracted spectra was also created.

### 3. SPECTRAL CATALOG

Because of the low metallicity of WLM classical MK spectral type indicators for early-type stars need to be adjusted in order to maintain a meaningful relation between spectral type and stellar physical properties as the strength of the metal lines becomes very low. This is of course important when comparing the massive stellar content of different galaxies, and is crucial for the work carried out in the Araucaria Project, that comprises galaxies of vastly different metallicities, spanning roughly one order of magnitude in Fe/H.

A number of authors have considered the classification of stars that are metal deficient relative to the Galactic MK standards. While the classification of O stars relies essentially on the He II-He I ionization equilibrium, and is therefore independent of metallicity, for B stars the classification relies on trends in the strength of metal lines, mostly from silicon and magnesium, and in the case of the later B-types these are measured in relation to He I features. Fitzpatrick (1991) showed how to transfer the MK classification framework to the B supergiants in the moderately metal-poor environment of the Large Magellanic Cloud (LMC), where the strengths of the spectral metal features are reduced by  $\sim 30\%$  relative

to the Galactic standards. Similarly, Lennon (1997) considered the case of B supergiants in the Small Magellanic Cloud (SMC), where the effects of the metal deficiency on the spectral classification are more important than in the case of the LMC. A classification scheme for A supergiants in the SMC was more recently developed by Evans & Howarth (2003).

The weakness of the diagnostic lines in the WLM stellar spectra implies that good S/N is necessary for a reliable classification. In our case, this was achieved for most of the targets in set A (the typical S/N per pixel is larger than 50), while for set B in general we were only able to provide a rough estimate of the spectral type. We also found that for some objects in the latter set of spectra the contamination due to the presence of unresolved companions appears to be significant.

A further consideration about our spectroscopic data concerns their rather coarse spectral resolution, about  $5 \text{ \AA}$ , relative to the  $1\text{-}2 \text{ \AA}$  resolution attained in the Magellanic Cloud works mentioned above, as well as in widely used digital spectral catalogs of early-type stars (e.g. Walborn & Fitzpatrick 1990). The consequent blending affects some of the spectral features employed in the classification (e.g. Si IV  $\lambda 4116$  and He I  $\lambda 4121$  in early B stars). Moreover, the measurement of weak metal line equivalent widths is not feasible at this resolution, preventing us from carrying out quantitative tests on the trends of metal line strengths with spectral type. However, overall we are confident about the reliability of the derived spectral classes, since in general these trends can be estimated qualitatively with good accuracy, provided the S/N of the spectra is sufficiently high.

#### 3.1. Classification criteria: spectral classes

For the classification of B supergiants we adopted the criteria introduced by Lennon (1997), developed for supergiant spectra in the SMC, where the present-day metal content is comparable to that found for WLM. For A-type supergiants, we used instead the scheme introduced by Evans & Howarth (2003) in their study of SMC stars, i.e. we relied on the strength of the Ca II H and K lines, namely the ratio of the line depths Ca II K/(Ca II H + He). This classification method has the advantage of being based on strong metal lines, and can therefore be applied to spectra of low spectral resolution and low S/N. The interstellar component of the Ca II lines, that cannot be disentangled from the stellar component at our spectral resolution, is expected to play only a second-order effect on the measured ratio. We note the different philosophy behind these two classification criteria: while the B-supergiant classification scheme was introduced by Lennon (1997) in order to extend the relation between spectral type and effective temperature observed in the Galactic standards to lower metallicities, the solution proposed for A-supergiants by Evans & Howarth (2003) allows for a metallicity dependence of the spectral type-temperature relation.

Our sample also includes two O stars. For their classification we relied on the stellar atlas by Walborn & Fitzpatrick (1990), supplemented by information contained in Walborn (1971) and Walborn et al. (2000).

#### 3.2. Luminosity classes

The luminosity classification was based on the empirical relationship between the equivalent width of  $H\gamma$  ( $W_\gamma$ ) and the luminosity class derived for O9-F8 stars in the SMC by Azzopardi (1987). However, the value of  $W_\gamma$  for three A supergiants in set A exceeds the maximum value assigned to

TABLE 1  
WLM - SPECTROSCOPIC TARGETS

Slit number	R.A. (J2000)	Decl. (J2000)	V	V-I	Spectral Type	K/(H + He)	$W_\gamma$	S/N	$V_{\text{Helio}}$ (km/s)	Comments
(1)	(2)	(3)	(4)	(5)	(6)	(7)	(8)	(9)	(10)	(11)
Set A										
1	0:01:58.46	-15:24:33.5	20.89	1.50	G5 I	~ 1	~ 3	16	-187	
2	0:01:59.04	-15:24:42.6	20.16	0.09	A0 II	0.27	6.0	44	-186	SC 68
3	0:01:56.63	-15:25:01.2	21.05	1.15	G0 I	0.85	2.2	18	-168	
4	0:02:01.59	-15:25:26.9	20.22	0.07	A2 II	0.41	7.1	44	-163	
5	0:02:03.32	-15:25:52.5	19.41	-0.04	B8 Iab	0.17	2.9	64	-148	SC 45
6	0:01:56.16	-15:26:24.6	19.82	0.38	A7 Ib	0.94	7.2	49	-136	SC 51
7	0:01:58.12	-15:26:48.6	19.69	-0.18	B1.5 Ia	0.35	1.6	58	-135	SC 37
8	0:01:55.04	-15:26:59.9	19.59	-0.05	B3 Ib	0.31	3.0	60	-143	SC 55
9	0:01:57.21	-15:27:18.1	18.44	-0.06	B1.5 Ia	0.28	1.6	101	-128	SC 35
10	0:01:54.08	-15:27:45.7	19.34	-0.15	B0 Iab	0.19	2.3	68	-126	SC 26
11	0:01:59.97	-15:28:19.2	18.40	-0.18	O9.7 Ia	0.25	1.7	106	-123	SC 30
12	0:01:53.24	-15:28:39.7	17.98	0.06	B9 Ia	0.26	1.9	119	-118	SC 22
13	0:01:53.35	-15:28:52.2	19.94	-0.15	B2.5 Ib	0.18	2.7	52	-113	SC 21
14	0:01:59.58	-15:29:26.3	18.43	0.23	A2 II	0.52	6.2	96	-94	SC 15
15	0:02:00.53	-15:29:52.1	20.36	-0.22	O7 V(f)	0.16	2.2	47	-115	SC 14
16	0:01:57.90	-15:30:13.4	18.44	0.16	A2 Ia	0.35	2.4	96	-68	SC 10
17	0:02:00.83	-15:30:25.0	19.34	0.00	B5 Ib	0.19	2.8	67	-74	SC 9
18	0:01:59.63	-15:31:00.3	19.04	1.69	G2 I	~ 1	2.0	30	-73	SC 4
19	0:02:00.84	-15:31:16.0	18.62	1.62	G2 I	1.4	2.0	36	-90	SC 6
Set B										
1	0:02:05.16	-15:24:22.7	21.00	0.37	A2 II	0.38	7.6	21	-162	
2	0:02:04.38	-15:24:46.3	20.38	0.06	A2 Ia	0.38	2.0	27	-145	
3	0:01:55.69	-15:24:48.8	20.48	0.01	B5 II	0.24	3.6	28	-125	SC 58
4	0:01:59.89	-15:25:28.0	20.83	0.36	A5 II	0.81	10.0	19	-154	
5	0:02:00.03	-15:25:44.8	20.80	0.08	A0 II	0.25	5.0	23	-120	
6	0:01:56.37	-15:26:06.5	20.02	0.28	A2 II	0.37	8.7	29	-131	SC 52
7	0:01:57.17	-15:26:14.3	20.32	0.32	A3 II	0.56	7.0	25	-128	
8	0:01:56.75	-15:26:36.6	20.24	0.22	A3 II	0.65	6.5	28	-136	
9	0:02:01.93	-15:27:25.3	19.82	0.09	A0 II	0.27	5.5	35	-104	SC 42
10	0:01:53.21	-15:27:29.2	19.04	-0.12	B2 II	0.29	3.2	53	-103	SC 27
11	0:01:56.35	-15:27:58.4	19.75	0.17	A0 Iab	0.31	3.4	32	-108	
12	0:02:00.64	-15:28:29.9	18.77	0.26	A2 II	0.51	6.6	57	-118	SC 31
13	0:01:53.65	-15:28:29.9	18.92	-0.14	B1 Ia	0.20	1.8	57	-101	SC 23
14	0:01:56.46	-15:29:01.7	19.98	0.03	A0 Ib	0.19	4.2	32	-89	
15	0:02:00.05	-15:29:31.1	20.32	0.36	A5 II	0.77	7.2	28	-98	
16	0:01:58.75	-15:30:01.7	20.08	0.20	composite	0.15	4.7	29	-93	SC 12
17	0:02:00.21	-15:30:14.2	20.27	0.16	composite	<0.08	2.2	26	-81	
18	0:01:59.44	-15:30:46.9	21.23	0.18	composite	...	...	17	...	
19	0:02:00.50	-15:31:08.4	19.73	-0.12	B2 Ib	0.21	2.9	37	-87	

the lowest luminosity class (Ib) in Azzopardi's work. In these cases (stars A2, A4 and A14) we have therefore assigned a luminosity class II. This matches what one obtains using the luminosity criteria adopted by Evans et al. (2004) for A-type supergiants contained in their 2dF survey of the SMC (their Table 5). Most of the stars in set B, including two B-type stars, have  $W_\gamma$  larger than for Ib supergiants, and were similarly classified as luminosity class II objects.

### 3.3. Results

We were able to apply the criteria above for all stars in set A (excluding four late-type stars), but the quality of set B spectra is in many instances not sufficient for an accurate classification. In this case, we have either attempted to match the observed spectra with SMC supergiant templates (B stars), admittedly producing a rather uncertain classification, or used the Ca II K/(Ca II H + He) criterion (A stars). We could not converge on a single dominant spectral type for three objects in set B (B16-B18), therefore they are labeled as 'composite' in Table 1, where we summarize our results. For each

blue supergiant we include: celestial coordinates (columns 2 and 3; measured with reference to the system defined by the USNO-2.0 catalog), photometric data ( $V$  in col. 4 and  $V-I$  in col. 5), the spectral type (col. 6), the ratio Ca II K/(Ca II H + He) (col. 7), the equivalent width of  $H_\gamma$  ( $W_\gamma$ , col. 8), the mean S/N per pixel of the spectrum (col. 9), and the heliocentric velocity measured from the Balmer lines ( $V_{\text{Helio}}$ , col. 10). The SC number from Sandage & Carlson (1985), when available, is included in column 11. Given the low resolution of the spectra, the uncertainty in  $V_{\text{Helio}}$  is around 10-15 km s<sup>-1</sup>. However, we note that the radial velocity information that we obtain across the galaxy is consistent with the H I rotation curve measured by Jackson et al. (2004), with objects in the northern half approaching us relative to the systemic velocity of -122 km s<sup>-1</sup> (Koribalski et al. 2004), and the southern half receding.

In Fig. 3 and Fig. 4 we show the normalized spectra of all the blue supergiants in set A, organized by spectral type, and starting with the earliest types. The lower-quality spectra of set B are shown in Fig. 5.

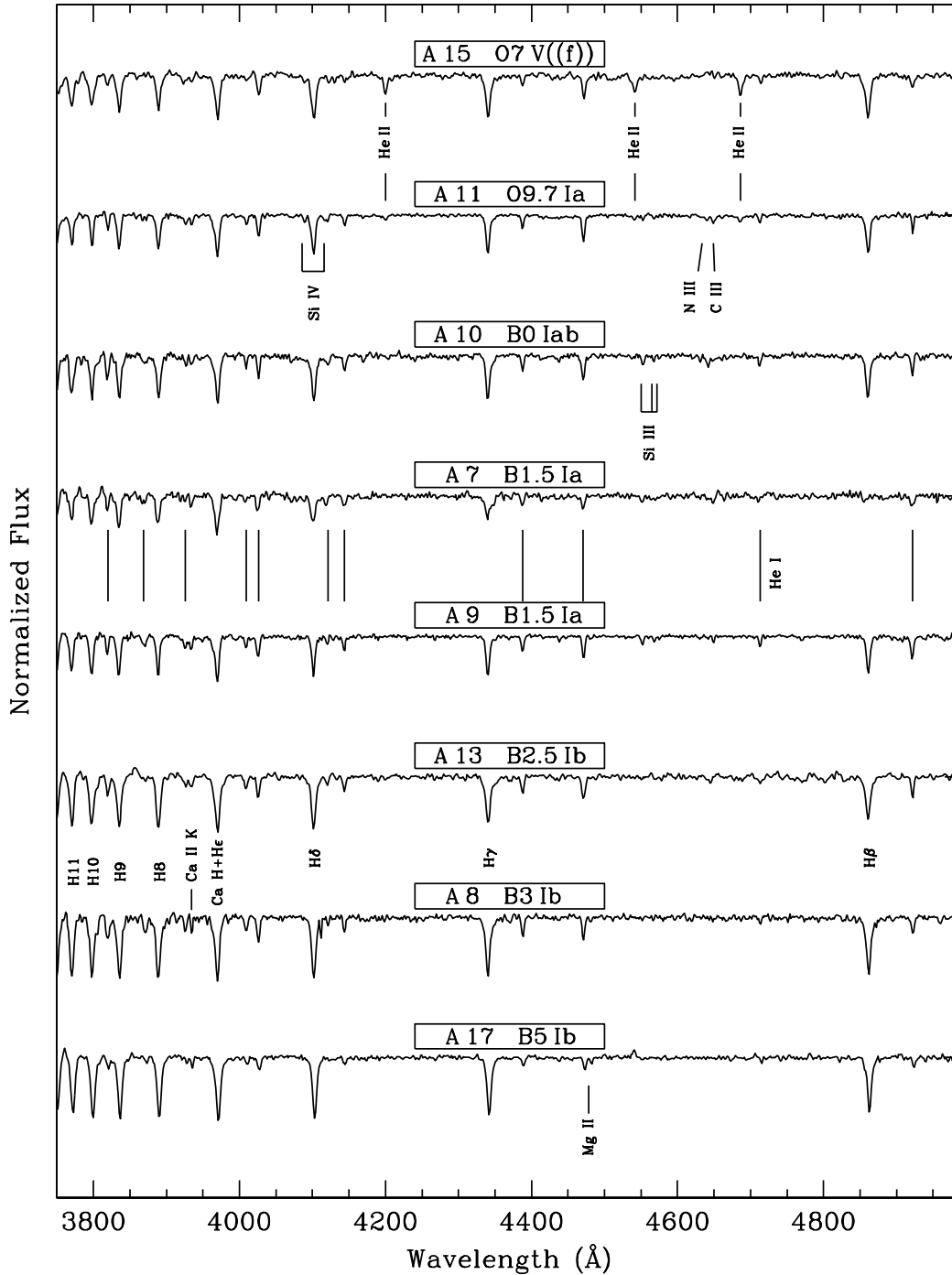


FIG. 3.— Normalized spectra of O and early-B supergiants in set A. The spectral features identified are: (*below A15*) He II  $\lambda\lambda 4200, \lambda 4542, \lambda 4686$ ; (*below A11*) Si IV  $\lambda\lambda 4089, \lambda 4116$ , N III  $\lambda\lambda 4634, 40-42$ , C III  $\lambda 4650$ ; (*below A10*) Si III  $\lambda\lambda 4553-68-75$ ; (*below A7*) He I  $\lambda 3820, \lambda\lambda 3867-72, \lambda 3926, \lambda 4009, \lambda 4026, \lambda 4121, \lambda 4144, \lambda 4388, \lambda 4471, \lambda 4713, \lambda 4922$ ; (*below A13*) Balmer lines from H $\beta$  to H11, and the Ca II K ( $\lambda 3933$ ) and H ( $\lambda 3968$ ) lines; (*below A17*) Mg II  $\lambda 4481$

As we remarked above, the classification criteria adopted here for A-type supergiants allow for a variation of stellar  $T_{\text{eff}}$  as a function of metallicity for a given spectral type, i.e. the spectrum of a star of low metallicity could resemble that of a *hotter* star of higher metallicity, because of the reduced strength of the metal features. This explains the different classification obtained for SC 15 and SC 31 by us (A2) and Venn et al. (2003) (A5), since the latter authors prefer to assign spectral types based on the measured temperature and a

$T_{\text{eff}}$ -spectral type relation valid for Galactic A supergiants.

We also note that the estimation of the stellar luminosity from the equivalent width of the Balmer lines can lead to apparently inconsistent results. This can be seen, for example, by comparing stars A14 and A16. These are both A2 stars, with virtually equal  $V$  magnitudes ( $V = 18.4$ ), but the former is classified as a luminosity class II object, based on its large  $W_{\gamma} = 6.2$ , while the latter is a class Ia star having  $W_{\gamma} = 2.4$ . Another luminosity class II A2 star, our object A4 in Table 1,

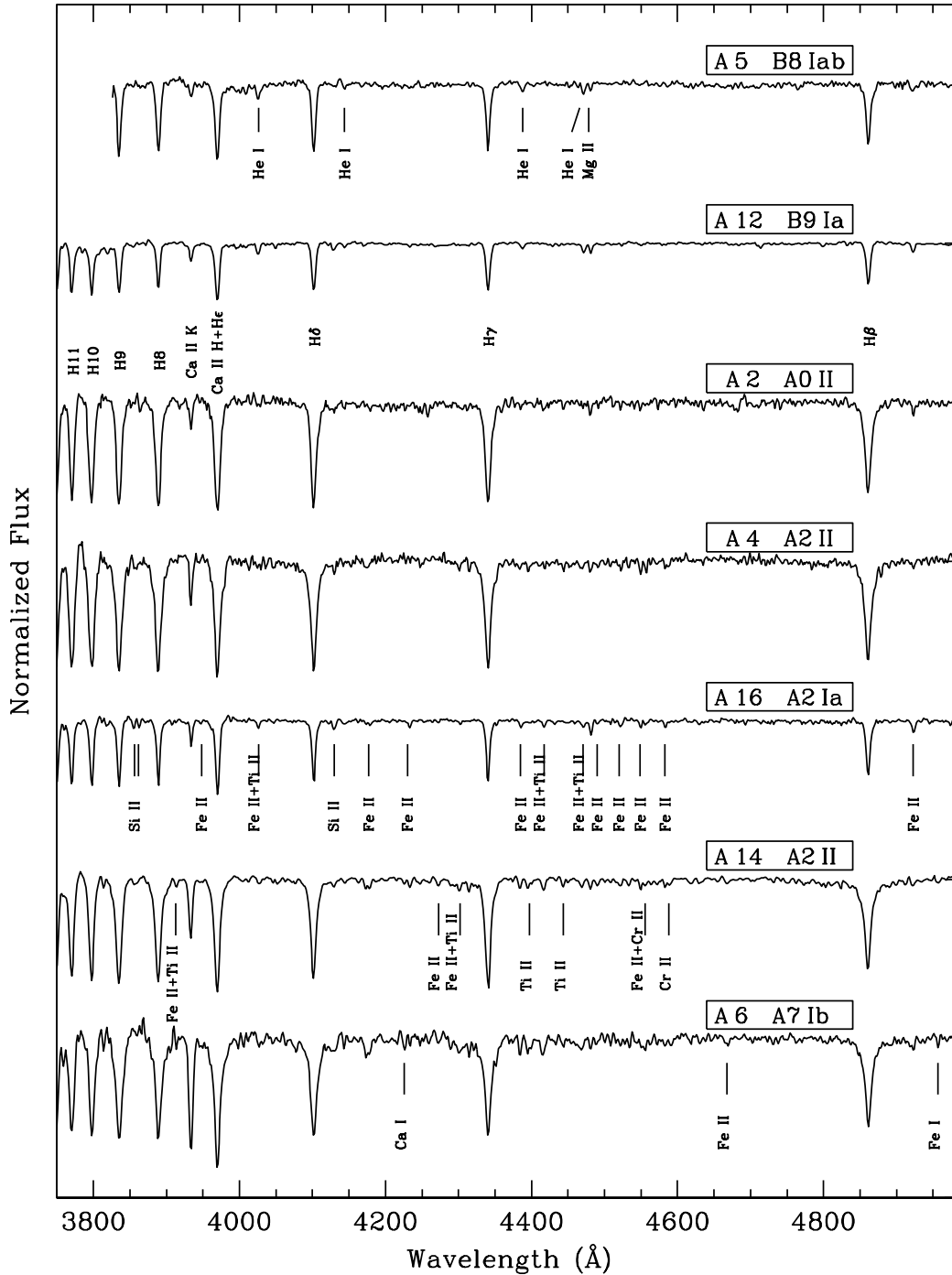


FIG. 4.— Normalized spectra of late-B and A supergiants in set A. The spectral features identified are: (*below A5*) He I  $\lambda\lambda 4026, \lambda\lambda 4121, \lambda\lambda 4388, \lambda\lambda 4471, \text{Mg II } \lambda\lambda 4481$ ; (*below A12*) Balmer lines from  $H\beta$  to H11, and the Ca II K ( $\lambda 3933$ ) and H ( $\lambda 3968$ ) lines; (*below A16*) Si II  $\lambda\lambda 3856-62, \lambda\lambda 4128-32, \text{Fe II } \lambda\lambda 3945, \lambda\lambda 4024, \lambda\lambda 4173-78, \lambda\lambda 4233, \lambda\lambda 4385, \lambda\lambda 4417, \lambda\lambda 4473, \lambda\lambda 4489-91, \lambda\lambda 4549, \lambda\lambda 4583, \lambda\lambda 4923, \text{Ti II } \lambda\lambda 4028, \lambda\lambda 4418, \lambda\lambda 4469-71$ ; (*below A14*) Fe II  $\lambda\lambda 3914, \lambda\lambda 4273, \lambda\lambda 4303, \lambda\lambda 4556, \text{Ti II } \lambda\lambda 3913, \lambda\lambda 4300, \lambda\lambda 4395-99, \lambda\lambda 4444, \text{Cr II } \lambda\lambda 4588, \lambda\lambda 4559$ ; (*below A6*) Fe II  $\lambda\lambda 4666-69, \text{Fe I } \lambda\lambda 4957, \text{Ca I } \lambda\lambda 4226$

is more than 1.5 magnitudes fainter. With the adopted value of the distance to WLM, and accounting for the small extinction towards it, stars A14 and A16 have an absolute magnitude  $M_V \simeq -6.6$ . According to the Galactic  $M_V$ -luminosity class calibration by Humphreys & McElroy (1984) these two stars would be classified as Iab supergiants, while A4 would be classified as Ib (other calibrations we considered would yield the same results). We note that the standard deviation in the Humphreys & McElroy (1984) calibration is typically 0.5

magnitudes for a given luminosity class. A large scatter in  $W_\gamma$  within a given luminosity class at fixed spectral type has also been noted more recently by Evans et al. (2004), who decided to use the information on the stellar brightness to define the luminosity class. In our case, however, rather than trying to adjust our luminosity classes from the knowledge of the absolute magnitude of the stars we will keep basing our stellar classification on the spectral morphology alone.

Foreground contamination is expected to be negligible for

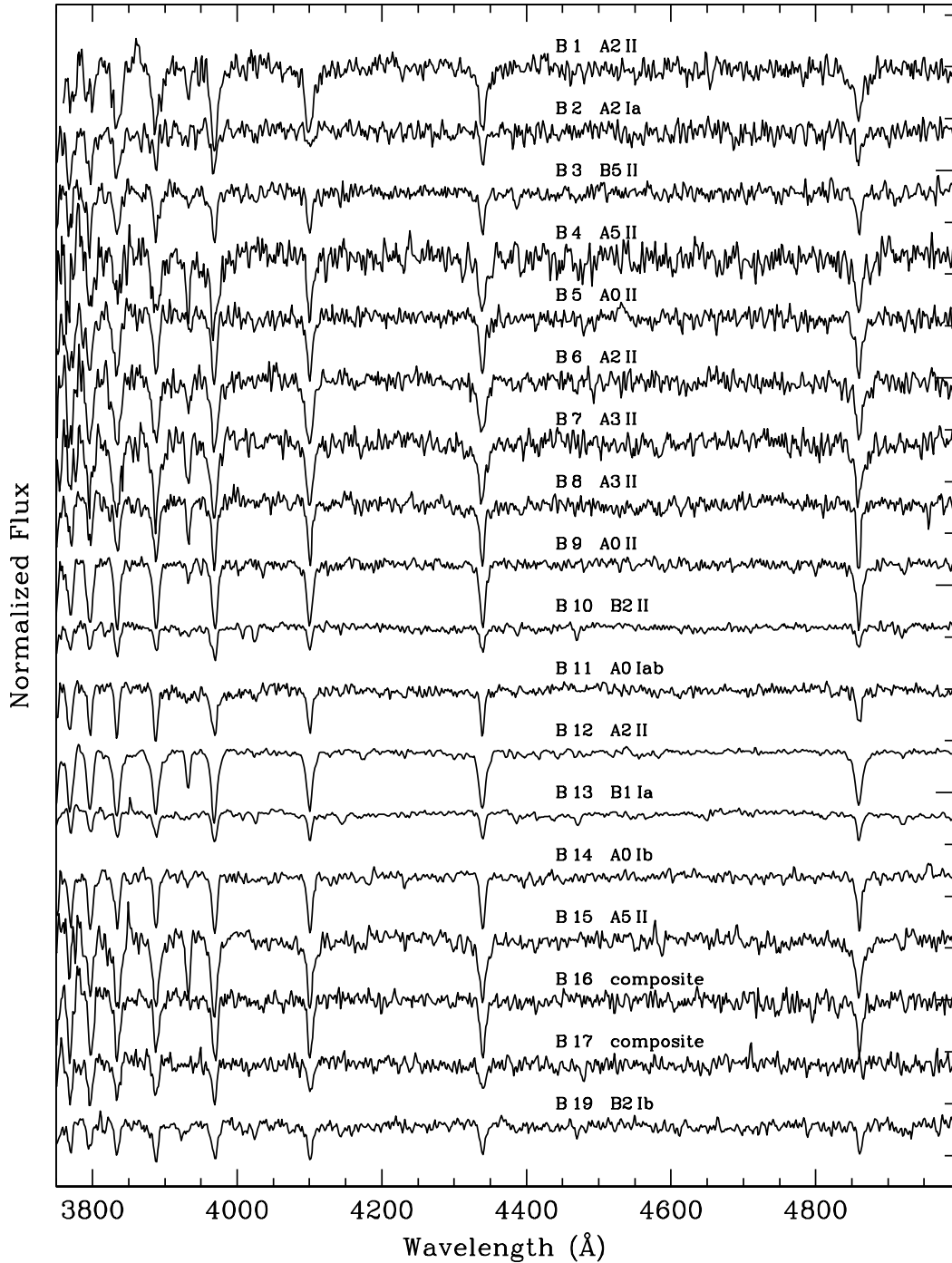


FIG. 5.— Normalized spectra for set B. The dominant spectral type is indicated.

all spectral types of interest here at the galactic latitude of WLM ( $b = -73^\circ 6$ ), as confirmed by the predictions from the Besançon models (Robin et al. 2003). We have estimated that the contamination from foreground dwarfs and giants is 1.5% in the region of the color-magnitude diagram occupied by the G stars A18 and A19, and 0.2% for the fainter G stars A1 and A3. For blue stars (B and A types) enclosed in the region of the color-magnitude diagram  $18 < V < 21$ ,  $-0.4 < (V - I) < 0.4$  the calculated contamination is 0.01%.

### 3.4. Comments on individual stars

We motivate here the detailed classification of the OB stars contained in our set A, based on the criteria used by Lennon (1997) for SMC supergiants. For A supergiants this is not necessary, as we derived the spectral classes simply from the Ca II K/(Ca II H + He) ratio (Table 1):

A5.— The relative intensity of He I  $\lambda 4471$  and Mg II  $\lambda 4481$  is the main temperature discriminant for late-B supergiants. The two lines have approximately the same strength at B8,

and Mg II  $\lambda 4481$  becomes progressively stronger relative to He I  $\lambda 4471$  for B9 and early A types. For this star, we observe Mg II  $\lambda 4481 < \text{He I } \lambda 4471$ . In addition, He I  $\lambda 4144 > \text{He I } \lambda 4121$ . These conditions apply to B8 stars in the scheme by Lennon (1997).

A7.– We assigned a B1.5 class from the absence of He II  $\lambda 4686$  (present in the B0 and B1 types), the absence of Si IV  $\lambda 4116$  and the presence of Si IV  $\lambda 4089 \simeq \text{O II } \lambda \lambda 4072-76$ . We excluded types B2 or later since no Si IV lines could be detected. This star, together with the nearby A8, A9 and A10, lies in a diffuse nebulosity surrounding the group of bright stars associated with the H II regions HM8 and HM9 (complex C1 of Hodge & Miller 1995). The Balmer lines of these four stars are mildly affected by weak nebular emission. This could explain the filling of the H $\beta$  line and the Ia luminosity class deduced from  $W_\gamma$ , despite the rather faint  $V$  magnitude.

A8.– In the scheme by Lennon (1997), the Si III  $\lambda 4553 \sim \text{Mg II } \lambda 4481$  at B2.5. At the cooler B3 type Si III  $\lambda 4553 < \text{Mg II } \lambda 4481$ , as observed in this star. The Si III line disappears at B5.

A9.– The B1.5 classification derives from the simultaneous absence of Si IV  $\lambda 4116$  and presence of Si IV  $\lambda 4089 \leq \text{O II } \lambda \lambda 4072-76$ . A weak nebular emission affects the Balmer lines. Detailed stellar parameters and the metal content for this star, as well as for A10 and A11, are measured in Sect. 4.

A10.– The He II lines at 4200, 4542 and 4686 Å are all present in this star's spectrum, while He II  $\lambda 4542 < \text{Si III } \lambda 4553$ , corresponding to a B0 type. The Balmer lines are affected by weak nebular emission.

A11.– The O9.7 type derives from the similarity in the strengths of He II  $\lambda 4542$  and Si III  $\lambda 4553$  (Walborn 1971). The ratios He II  $\lambda 4200/\text{He I } \lambda 4144$  and He II  $\lambda 4542/\text{He I } \lambda 4388$  are also consistent with the adopted spectral class.

A12.– Sandage & Carlson (1985) identified this as the visually brightest star in WLM. Our CCD magnitude,  $V = 17.98$ , corresponds to  $M_V \simeq -7.0$  when accounting for the foreground extinction. Note that this is more than 2 magnitudes fainter than the visually brightest blue stars (late-B to early-A supergiants, for which the bolometric corrections are small) found in more massive irregular galaxies, such as the Magellanic Clouds. We assign a B9 class from the conditions Mg II  $\lambda 4481 > \text{He I } \lambda 4471$  and Fe II  $\lambda 4233 < \text{Si II } \lambda \lambda 4128-32$ .

A13.– The Si IV lines are absent in this star, implying a type later than B1.5. Although the metal line strengths are uncertain at the FORS resolution and with the S/N of the observed spectrum, the Si III  $\lambda 4553$  is comparable to Mg II  $\lambda 4481$ , which indicates a type close to B2.5. The presence of Si III  $\lambda 4553$  excludes a type later than B3.

A15.– The main spectral type indicator for O stars is the ratio of He I  $\lambda 4471$  to He II  $\lambda 4542$ . For this star, the He I line is slightly stronger than the He II line. This is also true for He I  $\lambda 4026$  relative to He II  $\lambda 4200$ . The Si IV  $\lambda 4089$  is well detected. These criteria point to

a O7 type, or perhaps a slightly later type. If we use  $\log W' = \log W(4471) - \log W(4542) \simeq 0.0$ , we arrive at the same conclusion (Conti & Alschuler 1971). The weak N II  $\lambda \lambda 4634, 4640-42$  emission is associated with strong He II absorption, therefore the ((f)) designation. The V luminosity class derives from the strong He II  $\lambda 4686$  in absorption.

A17.– The Si III lines are absent (type  $\geq \text{B5}$ ), with Mg II  $\lambda 4481 < \text{He I } \lambda 4471$  (type  $\leq \text{B8}$ ). The relative strength of Si II  $\lambda \lambda 4128-32$  and He I  $\lambda 4121$  is used to distinguish the B5 and B8 classes. However, in our spectrum these two lines are very weak and have apparently the same strength. Somewhat arbitrarily we assign a B5 classification from the fact that the He I  $\lambda 4471/\text{Mg II } \lambda 4481$  ratio is larger than in our other B8 star (A5).

*G-type stars.*– Four objects in Table 1 (not shown in Fig. 3-4) have been classified as G stars. We have used the criteria in Evans & Howarth (2003): G-band/ $H_\gamma \simeq 0.9$  for G0 (star A3),  $H_\gamma > \text{Fe I } \lambda 4325$  for G2 (A18, A19) and  $H_\gamma \simeq \text{Fe I } \lambda 4325$  for G5 (A1). The negligible foreground contamination and the measured radial velocities, that indicate that these stars participate to the galactic rotation (see Table 1), strongly support the association of these four stars with WLM.

#### 4. B-STAR ABUNDANCES

The case of WLM is peculiar among dwarf irregular galaxies of the Local Group, in that the stellar oxygen abundance obtained for one A-type supergiant (A14=SC 15) is about five times larger than measured in H II regions:  $[\text{O}/\text{H}] = -0.21$  (Venn et al. 2003), corresponding to  $12 + \log(\text{O}/\text{H}) = 8.45$  when adopting the solar value  $12 + \log(\text{O}/\text{H})_\odot = 8.66$  (Asplund et al. 2004). The abundance of magnesium, also an  $\alpha$ -element, relative to the solar value determined from SC 15 and an additional A-type supergiant, SC 31 (=B12) is however 2.5 times lower than that of oxygen,  $[\text{Mg}/\text{H}] = -0.62$ . This is marginally consistent with the nebular oxygen abundance,  $[\text{O}/\text{H}] = -0.83$  [ $12 + \log(\text{O}/\text{H}) = 7.83$ ] measured by Lee et al. (2005).

Since both BA-type supergiants and H II regions are young objects, they should share a common chemical composition. The result found for oxygen in SC 15 is therefore puzzling. While a few explanations for the discrepancy between the nebular and the stellar oxygen abundance observed in WLM have been proposed by Venn et al., it is desirable to seek a comparison between stellar and nebular abundances using additional stars, in particular early-B stars, whose spectra contain a large number of O II lines (for A supergiants the measurement of the oxygen abundance relies on a single line, O I  $\lambda 6158$ ). We present here chemical abundances measured for three early-B supergiants, and we postpone the results for late-B and A stars to a future publication.

We have focused on the three brightest O/early-B stars: A9 (=SC 35, B1.5 Ia), A10 (=SC 26, B0 Iab) and A11 (=SC30, O9.7 Ia). The technique we employed for the abundance analysis of B supergiant spectra at FORS resolution has been explained in detail elsewhere (Urbaneja et al. 2003, 2005b). Stellar parameters and metal abundances are derived via comparisons with model spectra calculated with the FASTWIND code (Santolaya-Rey et al. 1997, Puls et al. 2005). The effective temperature is obtained from the silicon ionization balance (Si II/Si III and/or Si III/Si IV) or, in the case of the late-O star A11, the helium ionization balance (He I/He II). The

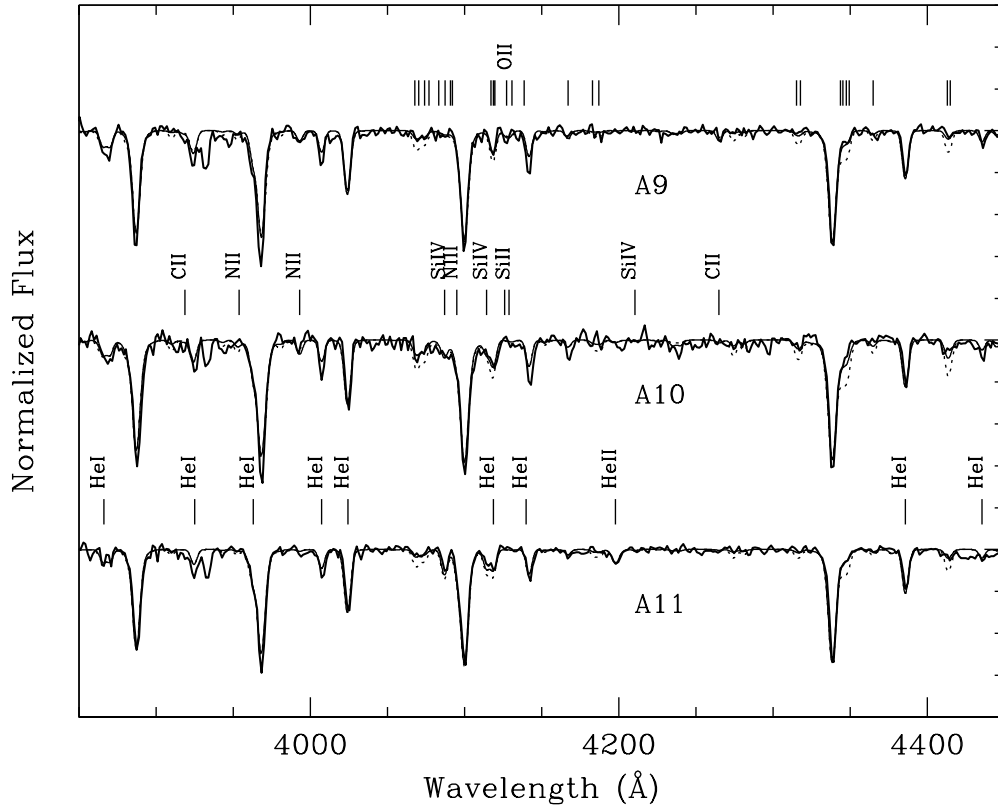


FIG. 6.— Comparison between the observed spectrum of the B-type supergiants A9, A10 and A11 (thick lines) with the best-fitting models (thin lines) in the 3850–4550 Å range. The dotted lines represent FASTWIND models calculated for a metallicity scaled up to the oxygen abundance measured by Venn et al. (2003),  $12 + \log(\text{O}/\text{H}) = 8.45$ . The line identification provided for O II lines (top), additional metal lines (center) and He I lines (bottom) refers to some of the strongest present.

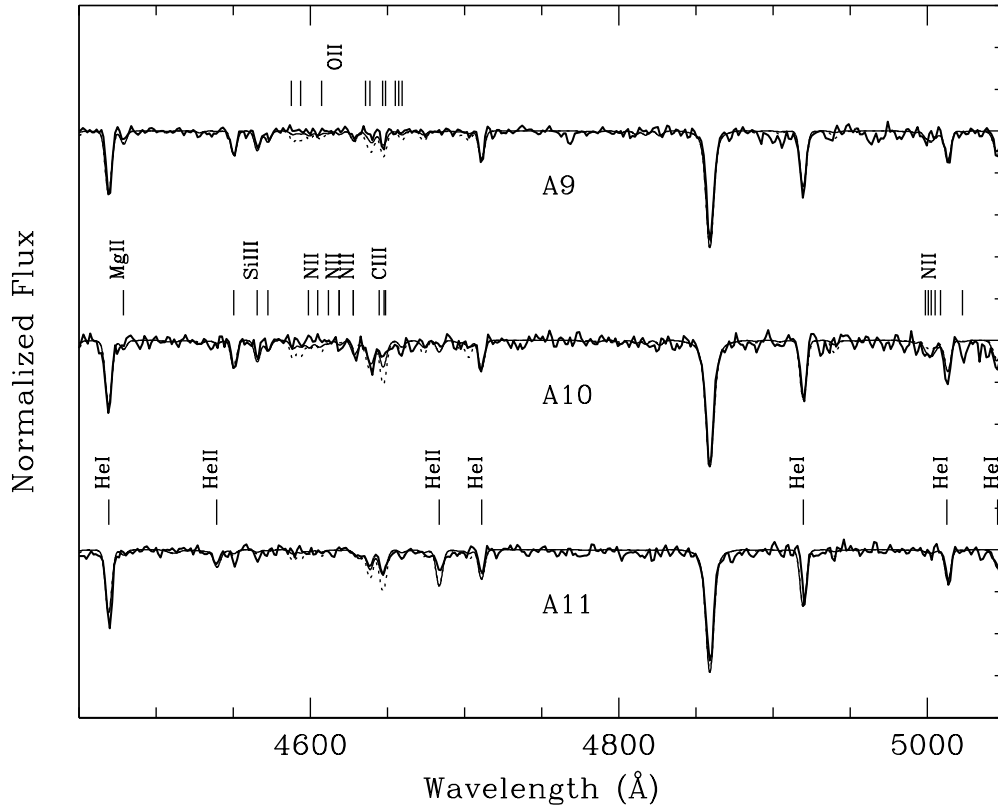


FIG. 7.— As Fig. 6, for the wavelength range 4550–5050 Å.

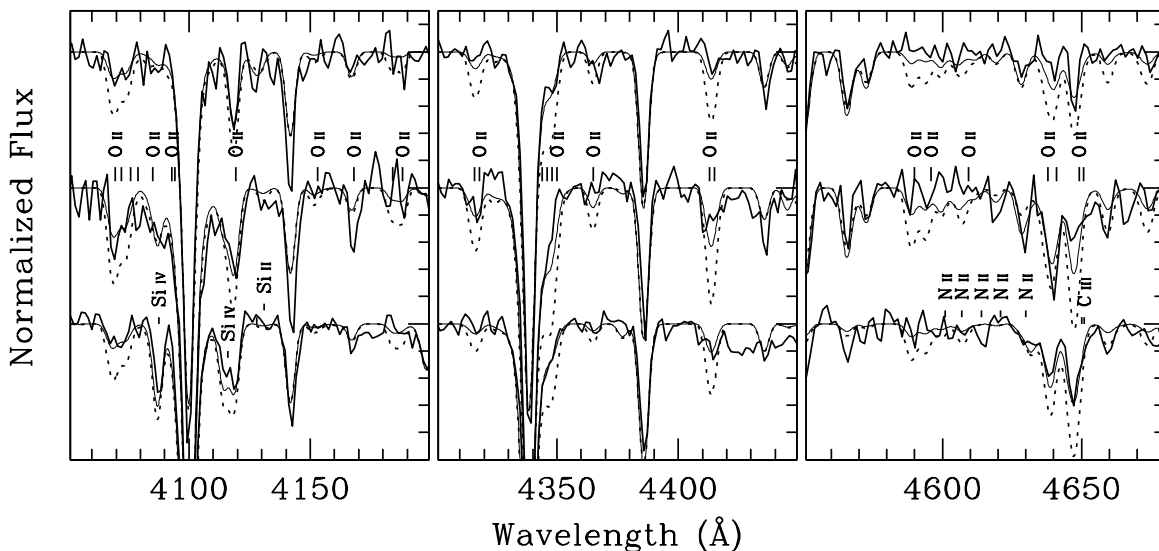


FIG. 8.— Enlargement of three portions of the spectra and models presented in Fig. 6-7, zooming in on prominent O II features. The observed spectra of A9 (top), A10 (middle) and A11 (bottom) are shown with thick lines, the models calculated with our adopted oxygen abundances and  $12 + \log(\text{O}/\text{H}) = 8.45$  are given by the thin and dashed lines, respectively.

surface gravity is obtained from fits to the hydrogen Balmer lines.

In order to determine the abundance of metals the principal features we rely on are: O II  $\lambda\lambda 4072-76$ , O II  $\lambda\lambda 4317-19$ , O II  $\lambda\lambda 4414-16$ , N II  $\lambda 3995$ , N II  $\lambda 5050$  (blend), C II  $\lambda 4267$ , Mg II  $\lambda 4481$ , Si II  $\lambda\lambda 4128-32$ , Si III  $\lambda\lambda 4553-68-75$  and Si IV  $\lambda\lambda 4089, 4116$ . However, there are a large number of metal features present in the spectra of early-B stars, especially due to O and N. At low spectral resolution we cannot base our abundance estimates on single metal features, therefore the abundance solution is obtained by attempting to reproduce as many spectral features as possible with the model spectra. This is especially critical for stars of low metal content, as is the case here, because of the weakness of the lines. Our estimated uncertainties are 1000 K on  $T_{\text{eff}}$ , 0.1 dex on  $\log g$  and 0.2 dex on the metal abundances (for details see Urbaneja et al. 2005b). Helium abundances are based on He I  $\lambda\lambda 4026$ ,  $\lambda 4388$ ,  $\lambda 4471$ ,  $\lambda 4921$ ,  $\lambda 5015$ ,  $\lambda 5048$  and  $\lambda 6678$ . The additional helium lines present in the spectra are not considered in the helium abundance calculation because of uncertainties in the corresponding Stark broadening data. These lines are nevertheless included in the model fits presented below.

In Fig. 6 and 7 we show with continuous thin lines our adopted fits to the spectra of A9, A10 and A11 (thick lines), in the wavelength intervals 3850-4450 Å and 4450-5050 Å, respectively. In these figures the dotted lines represent FASTWIND models in which the oxygen abundance was raised to the value measured by Venn et al. (2003),  $12 + \log(\text{O}/\text{H}) = 8.45$  in SC 15. As these figures and the enlargements in Fig. 8 show, such a high value is ruled out by comparing the observed and calculated strengths of several oxygen lines and line blends, e.g. those present in the red wing of H $\gamma$  at  $\lambda 4340$  Å, O II  $\lambda\lambda 4072-76$  and O II  $\lambda\lambda 4414-16$ .

The derived stellar parameters and chemical abundances are summarized in Table 2. For the parameters that are distance-dependent, we have assumed a distance to WLM of 0.93 Mpc ( $m - M = 24.85$ , McConnachie et al. 2005). The reddening has been obtained from a comparison of

TABLE 2  
B SUPERGIANTS - BEST FIT PARAMETERS

Properties	A9	A10	A11
Spectral type ...	B1.5 Ia	B0 Iab	O9.7 Ia
$T_{\text{eff}}$ (K).....	$20000 \pm 1000$	$25000 \pm 1000$	$29000 \pm 1000$
$\log g$ (cgs).....	$2.45 \pm 0.10$	$2.90 \pm 0.10$	$3.00 \pm 0.10$
$R/R_{\odot}$ .....	$39 \pm 2$	$20 \pm 2$	$26 \pm 2$
B.C.....	-1.91	-2.46	-2.83
$M_{\text{bol}}$ .....	$-8.58 \pm 0.13$	$-8.15 \pm 0.14$	$-9.33 \pm 0.13$
$\log L/L_{\odot}$ .....	$5.33 \pm 0.14$	$5.16 \pm 0.14$	$5.63 \pm 0.13$
$M^{\text{spec}}/M_{\odot}$ .....	$14 \pm 6$	$11 \pm 5$	$23 \pm 9$
$E(B-V)$ .....	0.06	0.04	0.04
$v_{\text{turb}}$ (km s $^{-1}$ )....	12	15	15
$Y_{\text{He}}$ .....	0.12	0.12	0.15
$\epsilon_{\text{C}}$ .....	7.4	< 6.9	< 6.9
$\epsilon_{\text{N}}$ .....	7.4	7.8	7.4
$\epsilon_{\text{O}}$ .....	7.7	7.9	7.9
$\epsilon_{\text{Mg}}$ .....	< 7.0	< 7.0	< 7.0
$\epsilon_{\text{Si}}$ .....	7.0	7.0	6.6
[O/H] (dex).....	-1.0	-0.8	-0.8
[Mg/H] (dex)....	< -0.6	< -0.6	< -0.6
[Si/O] (dex).....	0.46	0.26	-0.14

the observed  $V - I$  color index with the value derived from the spectral energy distribution of the best-fit models. In all three cases  $E(B - V)$  is consistent with a very small or a negligible component in addition to the foreground [ $E(B - V) = 0.035$ , Schlegel et al. 1998]. The metal lines in these spectra are in general very weak, and only upper limits on the abundances of some elements can be provided, as in the case of magnesium and carbon. For magnesium we obtained  $[\text{Mg}/\text{H}] < -0.6$ . The result from Venn et al. (2003) for two A supergiants is  $[\text{Mg}/\text{H}] = -0.62$ .

*Oxygen.*— The oxygen abundance we measure for the three stars we have analyzed is in the range  $12 + \log(\text{O}/\text{H}) = 7.7 - 7.9$ . The spread is within our uncertainties. Therefore, combining the three stars we derive a mean oxygen abundance  $12 + \log(\text{O}/\text{H}) = 7.83 \pm 0.12$ . This value agrees

extremely well with the findings of Lee et al. (2005). Their average of direct, electron-temperature based abundances for two H II regions yields  $12 + \log(\text{O}/\text{H}) = 7.83 \pm 0.06$ . Two of our stars, A9 and A10, are positioned within  $\sim 1$  arcmin (270 pc in projection) south of one of the two nebulae, HM9. The A11 supergiant is located further away, 360-450 pc from both H II regions, HM9 and HM7, towards the east, but quite near ( $\sim 70$  pc in projection) the A-type supergiant analyzed in the SE region of WLM by Venn et al. (2003), SC 31. This proximity contributes to make the hypothesis of chemical inhomogeneity in this part of WLM less likely (see the discussion at the end of this section).

*Nitrogen.*— The average abundance we measure is  $12 + \log(\text{N}/\text{H}) \simeq 7.5$ , the same value found by Venn et al. (2003) for SC 15. This is 1.2 dex higher than the average nitrogen abundance in the two H II regions studied by Lee et al. (2005). Considering the nebular value as the baseline for nitrogen in WLM, we therefore find an overabundance of nitrogen on the surface of the B-type supergiants of more than of a factor 10. From comparable overabundances observed in B-type supergiants in the SMC, Trundle & Lennon (2005) argue in support of the nitrogen enrichments predicted at the end of the core hydrogen burning phase by stellar evolution models that include rotational mixing (Maeder & Meynet 2001).

*Silicon.*— Our measured silicon abundances,  $12 + \log(\text{N}/\text{H}) = 6.6\text{--}7.0$  for the 3 different supergiants, are again in good agreement with the range of values determined in SC 15 and SC 31 by Venn et al. (2003),  $12 + \log(\text{N}/\text{H}) = 6.57\text{--}6.95$ . Since silicon is an  $\alpha$ -process element, its abundance is expected to follow that of oxygen. In our case,  $[\text{Si}/\text{O}]$  varies within a relatively wide range, between  $-0.14$  and  $0.46$ . We note, however, that a large scatter in the silicon abundance is also observed in other B-type supergiant samples, e.g. in the SMC (Lennon et al. 2003, Trundle et al. 2004) and M33 (Urbaneja et al. 2005a).

#### 4.1. UVES spectrum of A9

A high-resolution ( $R = 32000$ ) spectrum was obtained at the ESO VLT with UVES by Venn et al. (2003) for one of the B supergiants we have analyzed (A9 = SC35). This offered us the possibility of checking our abundance determinations for this star, and in particular to test whether the lower resolution of our FORS data affects the derivation of the chemical abundances. A 60-minute exposure resulted in a signal-to-noise ratio of about 50 per resolution element in the UVES spectrum. The wavelength coverage extends from 3800 Å to 10250 Å, but gaps are present around 4600 Å, 5600 Å and in the red. As a result, the spectrum of A9 lacks the Si III  $\lambda\lambda 4553\text{--}68\text{--}75$  lines, which are crucial  $T_{\text{eff}}$  diagnostic in the early-B spectral domain. For this reason, Venn et al. (2003) were not able to measure chemical abundances for this B supergiant.

During our analysis we did not carry out an independent abundance study for this star. Instead, we verified that the model spectrum calculated for the FORS data with the parameters found in Table 2 provides a good match to the spectral lines in the UVES data. The comparison between our model and the data is presented in Fig. 9, where we show the portions of the spectrum that contain the most important helium and metal features. We did not find it necessary to adjust the chemical abundances, and in particular we confirmed the low  $\alpha$ -element content of A9. The result of this test is important, because it further strengthens our

confidence in the abundances we are able to derive from spectra obtained with a resolution of 4-5 Å (Przybilla et al. 2006).

In conclusion, our results obtained for three supergiants do not substantiate the oxygen abundance discrepancy found by Venn et al. (2003) between H II regions and the A supergiant SC 15 (= A14). For other chemical species in common (N, Si, Mg), instead, we find similar abundances. The nebular and stellar oxygen abundances in WLM appear to be in excellent agreement, as previously found in other dwarf irregular galaxies of the Local Group, e.g. NGC 6822 (Venn et al. 2001) and Sextans A (Kaufer et al. 2004). This result confirms the peculiar nature of the star analyzed by Venn et al. (2003). Considering the different scenarios proposed by Venn et al. to explain this peculiarity, Lee et al. (2005) noted that the origin for the abundance discrepancy could be related to the location of SC 15 on the eastern side of the galaxy, where a peak in the H I distribution is found (Jackson et al. 2004), possibly connected with the presence of H II regions with enhanced extinction. This suggested unusual processes in this part of WLM (for example, dilution of the nebular chemical composition by metal-poor gas infall). However, we note that the SC 30 (= A11) supergiant analyzed in the current paper also lies in the same eastern region of the galaxy. From the B-star data presented here and from the available nebular abundances we do not find support for the presence of chemical spatial inhomogeneities in WLM.

#### 5. PHOTOMETRIC VARIABILITY

In our work on NGC 300 we found that about 20% of the blue supergiants we investigated spectroscopically in that galaxy are variable (Bresolin et al. 2004b). However, we concluded from the analysis of 14 B8-A2 supergiants with light amplitudes in the *V* band between 0.08 mag and 0.23 mag that the observed variability does not significantly affect the FGLR (Kudritzki et al. 2003). We have examined our multi-epoch photometry of the spectroscopic targets in WLM in order to verify the presence of variability. For most stars we have *V* photometry for approximately 100 epochs, extending over a period of more than two years (October 2001–December 2003). We have compared the standard deviation  $\sigma_V$  of the *V* magnitudes of the spectroscopic targets with that of the general stellar population in WLM, as shown in Fig. 10. Most of the stars for which we obtained spectra have  $\sigma_V$  that are consistent with the observational scatter of non-variable stars. Only three outliers are found: A18 (spectral type G2), A7 (B1.5 Ia) and A8 (B3 Ib), with  $\sigma_V \simeq 0.05$  mag. The variability of these three stars is significant at the  $2\text{--}3\sigma$  value. The analysis of their light curves did not reveal any significant periodicity, however. The star A18 (= SC 4) was identified as a red irregular variable by Sandage & Carlson (1985). In fact, it is the one with the largest amplitude in the *B*-band (0.69 mag) in their sample.

We conclude that most of the spectroscopic targets are non-variable stars, at least within the limits of our photometric accuracy. The absence of variability at the 0.1 mag level or more for all the spectroscopic targets implies that even in the case of WLM the photometric variability is not a cause for concern in the determination of the FGLR.

#### 6. SUMMARY AND CONCLUSIONS

As part of our photometric and spectroscopic investigation of the stellar content of nearby galaxies, the Araucaria Project, we have presented the first extensive spectral catalog of stars

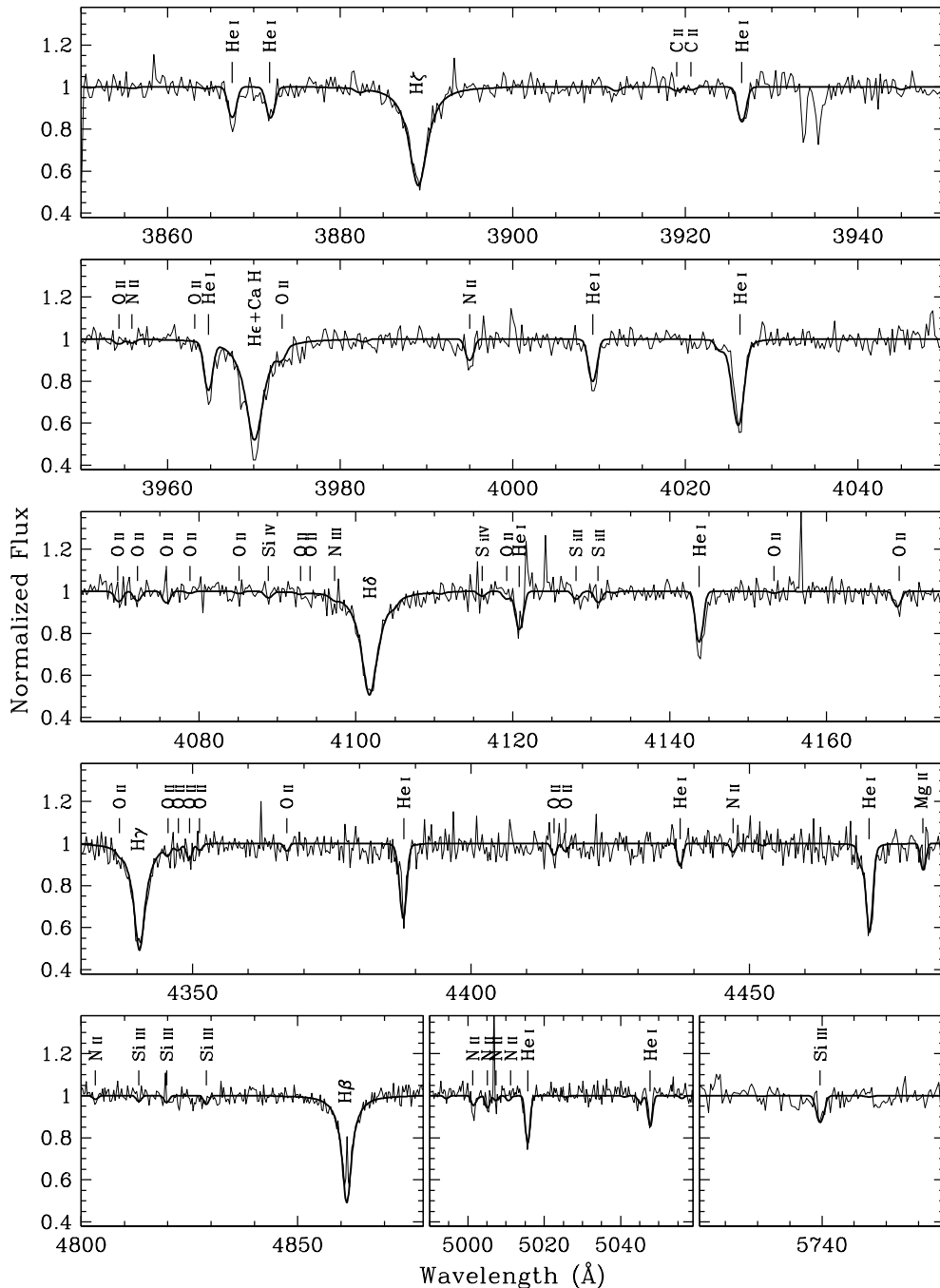


FIG. 9.— The UVES spectrum of the B1.5 Ia supergiant A9 (thin line) is compared to a FASTWIND model calculated with the stellar parameters and chemical abundances derived from the FORS spectrum, and summarized in Table 2. We show here the portions of the spectrum containing the most important metal features, labeled in the top half of each panel.

in the dwarf irregular galaxy WLM. In our series of papers focused on the analysis of blue supergiants, our first step involves the classification of the available spectra, since it provides a first order approach to the physical characteristics of the target stars. In the case of WLM, as well as in additional dwarf irregulars that are part of the project and that will be considered in future publications (e.g. IC 1613 and NGC 6822), this process needs to account for the low metal content of the galaxy relative to the galactic standards used in the MK process. We have therefore based our spectral classification on the criteria developed for B and supergiants con-

tained in the Small Magellanic Cloud by Lennon (1997) and Evans & Howarth (2003), respectively.

Our spectral catalog, presented in Table 1 and in Fig. 3-5, shows that our higher S/N spectroscopic sample of 19 objects, selected from VI photometry, contains at least 6 early-B (B0-B5) supergiants and 6 late-B and early-A (B8-A2) stars of luminosity class between Ia and II, as well as an O7 V star and an O9.7 Ia star. The spectra of several of these stars is of sufficient quality for a determination of the stellar parameters and abundances. We have acquired also a second set of lower S/N spectra for mostly BA stars, however their quality

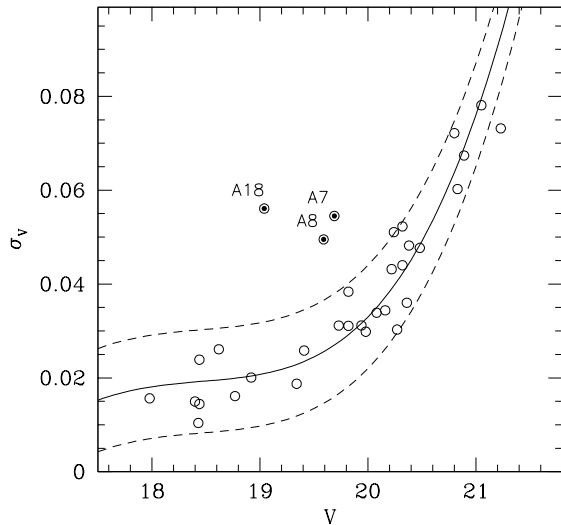


FIG. 10.— The standard deviation in the V band,  $\sigma_V$ , from measurements at approximately 100 epochs, is shown as a function of V magnitude for 33 of the spectroscopic targets (open circles). The trend of the median value for nearly 5000 stars in WLM is shown with the continuous line. The dashed lines are drawn at the approximate  $1\text{-}\sigma$  deviation from the median (0.11 mag). The three outliers A7, A8 and A18 are indicated with the different symbols.

in general does not allow us to carry out further analysis.

We have carried out a quantitative analysis for three of our targets: A9 (B1.5 Ia), A10 (B0 Iab) and A11 (O9.7 Ia). Using FASTWIND models we have derived chemical abundances

for oxygen, nitrogen and silicon, while upper limits were estimated for carbon and magnesium. The oxygen abundance for the three supergiants is consistent with a single value corresponding to  $12 + \log(\text{O}/\text{H}) = 7.83 \pm 0.12$ . This oxygen abundance is in excellent agreement with the measurement derived from H II regions. Our one B-supergiant spectrum in the SE region does not confirm the high oxygen abundance from the A-type supergiant in this region. From our B-supergiant analysis the SE region could thus have the same oxygen abundance as the rest of WLM.

In addition to the measurement of chemical abundances in blue supergiants, we are focusing on the use of these stars as extragalactic distance indicators, through the Flux-weighted Gravity–Luminosity Relationship (FGLR). The FGLR for supergiants in WLM will require the determination of stellar parameters for a larger sample of objects, and will be presented in an upcoming publication. Here we have shown that a possible complication in the FGLR method, namely the photometric variability of the target stars, is negligible, confirming our previous conclusion (Bresolin et al. 2004b) that the FGLR is insensitive to the microvariability of blue supergiants.

We thank L. Rizzi for help in the astrometric calibration of the FORS2 WLM image. GP and WG gratefully acknowledge financial support from the Chilean Center for Astrophysics FONDAP 15010001.

#### REFERENCES

- Asplund, M., Grevesse, N., Sauval, A. J., Allende Prieto, C., & Kiselman, D. 2004, *A&A*, 417, 751
- Azzopardi, M. 1987, *A&AS*, 69, 421
- Bresolin, F., Kudritzki, R.-P., Mendez, R. H., & Przybilla, N. 2001, *ApJ*, 548, L159
- Bresolin, F., Gieren, W., Kudritzki, R.-P., Pietrzyński, G., & Przybilla, N. 2002, *ApJ*, 567, 277
- Bresolin, F., Garnett, D. R., & Kennicutt, R. C. 2004a, *ApJ*, 615, 228
- Bresolin, F., Pietrzyński, G., Gieren, W., Kudritzki, R.-P., Przybilla, N., & Fouqué, P. 2004b, *ApJ*, 600, 182
- Bresolin, F., Schaerer, D., González Delgado, R. M., & Stasińska, G. 2005, *A&A*, 441, 981
- Conti, P. S. & Alschuler, W. R. 1971, *ApJ*, 170, 325
- Dolphin, A. E. 2000, *ApJ*, 531, 804
- Evans, C. J. & Howarth, I. D. 2003, *MNRAS*, 345, 1223
- Evans, C. J., Howarth, I. D., Irwin, M. J., Burnley, A. W., & Harries, T. J. 2004, *MNRAS*, 353, 601
- Ferraro, F. R., Fusi Pecci, F., Tosi, M., & Buonanno, R. 1989, *MNRAS*, 241, 433
- Fitzpatrick, E. L. 1991, *PASP*, 103, 1123
- Gieren, W., Pietrzyński, G., Bresolin, F., Kudritzki, R.-P., Minniti, D., Urbaneja, M., Soszyński, I., Storm, J., Fouque, P., Bono, G., Walker, A., & García, J. 2005, *The Messenger*, 121, 23
- Hodge, P. & Miller, B. W. 1995, *ApJ*, 451, 176
- Humphreys, R. M. & McElroy, D. B. 1984, *ApJ*, 284, 565
- Jackson, D. C., Skillman, E. D., Cannon, J. M., & Côté, S. 2004, *AJ*, 128, 1219
- Kaufer, A., Venn, K. A., Tolstoy, E., Pinte, C., & Kudritzki, R.-P. 2004, *AJ*, 127, 2723
- Koribalski, B. S. et al. 2004, *AJ*, 128, 16
- Kudritzki, R. P., Bresolin, F., & Przybilla, N. 2003, *ApJ*, 582, L83
- Lee, H., Skillman, E. D., & Venn, K. A. 2005, *ApJ*, 620, 223
- Lee, M. G., Freedman, W. L., & Madore, B. F. 1993, *ApJ*, 417, 553
- Lennon, D. J. 1997, *A&A*, 317, 871
- Lennon, D. J., Dufton, P. L., & Crowley, C. 2003, *A&A*, 398, 455
- Maeder, A. & Meynet, G. 2001, *A&A*, 373, 555
- McConnachie, A. W., Irwin, M. J., Ferguson, A. M. N., Ibata, R. A., Lewis, G. F., & Tanvir, N. 2005, *MNRAS*, 356, 979
- Minniti, D. & Zijlstra, A. A. 1996, *ApJ*, 467, L13+
- . 1997, *AJ*, 114, 147
- Pagal, B. E. J., Edmunds, M. G., Blackwell, D. E., Chun, M. S., & Smith, G. 1979, *MNRAS*, 189, 95
- Pietrzyński, G., Gieren, W., & Udalski, A. 2002, *PASP*, 114, 298
- Pietrzyński, G., Gieren, W., Udalski, A., Bresolin, F., Kudritzki, R.-P., Soszyński, I., Szymbański, M., & Kubiak, M. 2004, *AJ*, 128, 2815
- Przybilla, N., Butler, K., Becker, S. R., & Kudritzki, R. P. 2006, *A&A*, 445, 1099
- Puls, J., Urbaneja, M. A., Venero, R., Repolust, T., Springmann, U., Jokuthy, A., & Mokiem, M. R. 2005, *A&A*, 435, 669
- Rejkuba, M., Minniti, D., Gregg, M. D., Zijlstra, A. A., Alonso, M. V., & Goudfrooij, P. 2000, *AJ*, 120, 801
- Robin, A. C., Reylé, C., Derrière, S., & Picaud, S. 2003, *A&A*, 409, 523
- Sandage, A. & Carlson, G. 1985, *AJ*, 90, 1464
- Santolaya-Rey, A. E., Puls, J., & Herrero, A. 1997, *A&A*, 323, 488
- Schlegel, D. J., Finkbeiner, D. P., & Davis, M. 1998, *ApJ*, 500, 525
- Skillman, E. D., Kennicutt, R. C., & Hodge, P. W. 1989a, *ApJ*, 347, 875
- Skillman, E. D., Terlevich, R., & Melnick, J. 1989b, *MNRAS*, 240, 563
- Trundle, C., Dufton, P. L., Lennon, D. J., Smartt, S. J., & Urbaneja, M. A. 2002, *A&A*, 395, 519
- Trundle, C. & Lennon, D. J. 2005, *A&A*, 434, 677
- Trundle, C., Lennon, D. J., Puls, J., & Dufton, P. L. 2004, *A&A*, 417, 217
- Urbaneja, M. A., Herrero, A., Bresolin, F., Kudritzki, R.-P., Gieren, W., & Puls, J. 2003, *ApJ*, 584, L73
- Urbaneja, M. A., Herrero, A., Kudritzki, R.-P., Najarro, F., Smartt, S. J., Puls, J., Lennon, D. J., & Corral, L. J. 2005a, *ApJ*, 635, 311
- Urbaneja, M. A., Herrero, A., Bresolin, F., Kudritzki, R.-P., Gieren, W., Puls, J., Przybilla, N., Najarro, F., & Pietrzyński, G. 2005b, *ApJ*, 622, 862
- Venn, K. A., Lennon, D. J., Kaufer, A., McCarthy, J. K., Przybilla, N., Kudritzki, R. P., Lemke, M., Skillman, E. D., & Smartt, S. J. 2001, *ApJ*, 547, 765
- Venn, K. A., Tolstoy, E., Kaufer, A., Skillman, E. D., Clarkson, S. M., Smartt, S. J., Lennon, D. J., & Kudritzki, R. P. 2003, *AJ*, 126, 1326
- Walborn, N. R. 1971, *ApJS*, 23, 257
- Walborn, N. R. & Fitzpatrick, E. L. 1990, *PASP*, 102, 379
- Walborn, N. R., Lennon, D. J., Heap, S. R., Lindler, D. J., Smith, L. J., Evans, C. J., & Parker, J. W. 2000, *PASP*, 112, 1243